Materials Science Forum Vols. 173-174 (1995) pp. 319-324

A LASER SYSTEM FOR SILICON SOLAR CELL PROCESSING: DESIGN, SET-UP AND OPERATION

L. Pirozzi, U.B. Vetrella, M. Falconieri and E. Salza

ENEA, CRE Casaccia, via Anguillarese 301, I-00060 Roma, Italy

Keywords: High Efficiency Solar Cells, Texturing Doping

Abstract. In this paper we will show the results obtained by using a laser system in the fabrication process of mono and polycrystalline silicon solar cells. A laser system for silicon solar cell processing has been designed and assembled in our laboratories; this system consists of a Nd-YAG, 100 W multimode, 14 W single mode (TEM_{00}), Q-switched laser, and of an X-Y 2 μm resolution motorized table. The most important variables affecting the characteristics of the scribing process have been studied, concerning the mechanical and optical arrangement of the system. Several batches of samples have been processed and tested, in order to optimize these variables. Possible damages arising from the laser treatments have been fully investigated by optical and electrical measurements. Texturization of the cell surface by a cross-hatched pattern of parallel and perpendicular grooves was obtained by realizing a pyramidal structure on the silicon surface. We achieved reflectance values of about 10% and even lower numbers when a suitable single anti-reflecting coating (ARC) was superimposed to such a structure. A further step was the grooving of solar cells silicon surfaces to produce metal gridline patterns, in the laser grooved, buried contact, high efficiency solar cell structure. In this way we have determined the best conditions to obtain grooves with the desired depth and width, and with the cleanest and sharpest shape. Eventually, we have set up the laser assisted heavy doping of the grooves for achieving the selective emitter structure by using the second harmonic (532 nm) of the Nd-YAG laser.

INTRODUCTION.

In photovoltaic applications, laser scribing is widely used in large area amorphous silicon integrated panels fabrication /1/, and seems to be a feasible way in the preparation scribed contacts of Copper Indium Diselenide solar cells /2/. As far the most important photovoltaic material, that is mono and poly crystalline silicon, laser systems are used by some industries to carry out important processes, like silicon ribbon trimming or gridline patterning. When applied at laboratory level, silicon solar cells laser processing reached incredible results /3/.

We have set up in our laboratory a Nd-YAG laser system, with the aim of carrying out a systematic study of its possible applications in photovoltaics, and in particular in mono and poly crystalline silicon solar cells processing. We used this system to make gridline patterns for buried metal contacts, to get silicon surface texturization with a low effective reflectance, and to study laser-induced doping in a suitable reactive controlled atmosphere. Thorough investigations about any possible performance loss induced by the laser process was moreover carried out.

SYSTEM DESIGN.

A laser system for solar cell processing consists mainly of three parts:
1) a laser source;
2) the focusing optics;
3) a sample or beam motion apparatus electronically controlled.

The choice of every part must be done taking into account both the general frame of electronic devices laser processing and the particular applications envisaged.

1). As far the laser source is concerned, the most widely used system for silicon electronic devices processing is a Q-switched Nd-YAG source working in TEM00, due to the sufficient absorption coefficient of silicon at the emission wavelength 1064 nm (α=11.1 cm^{-1}), the short pulse duration, which leads to low thermal damage, and the high repetition rate, that allows high processing speed /4/. In particular, the specifications of our laser source are:

Laser	ND-YAG Q-switched
Wavelength	1064 nm
CW Power Multimode	40 Watt
CW Power TEM_{00}	14 Watt
Q-switched Power (1 KHz TEM_{00})	4 Watt
Pulse Width	100 nsec
Peak Power	40 KWatt
Beam Divergence	2.5 mrad

2). The choice of the focusing optics is related to the selection of the motion: beam motion requires a dynamic focusing system, while a fixed focus arrangement is sufficient if sample movements are selected. The latter option is more convenient for a laboratory level set up, taking into consideration that high precision, low cost, and simplicity are required. For these reasons, we choose a sample motion arrangement, so that our fixed focusing optics consists simply of a combined system made of interchangeable beam expanders and focusing objectives; the expansion ratio and the objective f/n being selected according to the particular application.

3). A computer controlled X-Y, DC operating table, with a total excursion of 140 mm and a resolution of 2 µm was used to move the sample under the beam; maximum speed is 50 mm/s. Table movements and laser switches were computer controlled, with the aid of suitable CAD software. The motorized table is positioned horizontally, placed at right angle with the laser, and a properly coated mirror is used to reflect the beam onto the sample; with this arrangement, we can avoid the use of any additional wafer holder, and we can follow real-time the process through a video camera placed vertically on the sample.

Further to this set up, the system was improved by adding a frequency doubler and a reaction chamber.

The green (532 nm) light has a penetration depth into the silicon of about 2 µm (α=8300 cm^{-1}), and permits a better focusing (by which we can get smoother grooves) and surface processes, such as laser induced doping. In our case the second harmonic of the fundamental 1064 nm Nd-YAG line is obtained by using an intra-cavity LBO crystal, cut at Brewster angle to minimize reflectance losses; a spatial selection of the doubled component only was made thanks to a system of prisms and mirrors properly coated and arranged. Maximum output power was 600 mW.

The reaction chamber has been realized to perform laser processes in a controlled atmosphere, such as laser induce doping. The chamber is made of high quality vacuum stainless steel in order to minimize desorptions from the walls and to be able to work with reactive gases, it has an O-ring seal and a quartz window on top; wafers up to 10x10 cm^2 can be held at a maximum temperature of 400 °C during the process. Pumping system has been designed to achieve a high vacuum value better than 10^{-5} mbar, and to be able to handle reactive gases used as dopants. The chamber is placed onto the motorized table, and every part of it is held at a suitable temperature, so to avoid any possible moist formation.

SYSTEM CHARACTERIZATION.

In order to determine the best working conditions, preliminary tests were performed on several samples of silicon with the aim to find out the influence of the laser parameters on the quality of the scribed patterns, and the presence of possible laser induced damages. This latter point is particularly important, as a laser assisted process does not seem to be free from drawbacks due to the basic mechanism of this process, based on the vaporization of the material.

Grooving set-up. Wafers used to characterize the system were commercially available monocrystalline and polycrystalline silicon; prior to the process, wafers were cleaned in a suitable chemical bath (HF, or HF+RCA). All the meaningful tests reported were performed at 1064 nm, spot size was 1.2 mm, lasing power was varied between 1.2 and 4.1 W.

To start with, we first determined the overlap value. Because Q-switching results in a series of discrete, high energy and short pulses, it is necessary to overlap pulses in order to create a continuous scribe line; after several trials, an overlap value of 75% was found as the best compromise between the speed and the quality of the lines; overlap values down to 50% were found to give satisfactory results anyway. We experimented also the effect of making the grooves by multiple passing: this option was rejected because of the too long time to draw a grid structure.

To keep the overlap to its optimum value, we used a repetition rate of 2000 Hz, and a slit translation speed of 10 mm/s; with these arrangement, the best shape and 'cleanness' of the grooves were obtained with two set-up: lens focus 27.2 mm, beam expander 6x; lens focus 46.4 mm, beam expander 10x.

After every test, groove characteristics were investigated by optical (Reichert-Young Polyvar Met) and scanning electron (SEM) microscopy. Results of these inspections are summarized in Table I.

By using the parameters reported above, grooves with a minimum widths in the range 25 to 35 micron and with a depth of about 60 micron were readily achievable.

From these measurements, we learned that 1064 nm line produces many silicon residues, deposited on the surface of the wafer and inside the grooves. To reduce the amount of this unwanted material, a nozzle was placed on the X-Y table, blowing air or nitrogen, and a suitable NaOH based etch was used to definitely clean the grooves after the process.

Differently, the use of the 532 nm green beam allowed grooves with a width of 20 μm and a depth of less than 25 μm; they appeared also very clean, with a limited presence of melted residues, so that a light chemical treatment was necessary.

We also processed wafers on which it was deposited an ARC layer, slight adjustments of the parameters around their optimal value were needed.

Laser induced damages. The effects of rapid thermal treatments and of thermal waves driven into the sample, in principle, could give origin to cell performances loss mainly through three mechanisms: creation of dislocations, creation of amorphous phases, diffusion of impurities due to chemical treatments.

To simulate dopant diffusion, after scribing, some wafers underwent a thermal treatment, 920 C for 30 minutes.

Laser induced damages were investigated by using Surface Photo Voltage (SPV) and Laser Beam Induced Current (LBIC) techniques. By using these measurements together with microscopy, we have been able to know not only the 'optical' width of grooves and the occurrence of any residue, but also their 'electrical' width and activity due to micro structural changes or impurity contamination, both induced by chemical or thermal treatments.

To carry out SPV measurements, thick polycrystalline wafers (t=1.2 mm) were measured with a large spot SPV equipment illuminating about 80% of the total wafer area, in order to determine the diffusion length /5/. Good quality material was chosen, with a measured starting diffusion length between 120 and 150 μm. After laser scribing, wafers were measured again, and no degradation was detected. The same measurements were repeated subsequently the high temperature step and HF removal of the surface oxide: no appreciable degradation of the diffusion length was observed this time either.

Our LBIC apparatus was equipped with three light beams with different wavelengths, namely 532 nm (doubled Nd-YAG laser), 632.8 nm (He-Ne laser), and 1064 nm (Nd-YAG laser), so to be able to probe the material at different depths; the minimum step and reproducibility of the x-y motorized system was 1 μm; dimensions of the beam spot could be made as small as 4 μm for He-Ne laser.

Results of LBIC scans gave no indication of detrimental effects induced by the laser process, by the chemical etch, or by the thermal treatment.

To summarize our set-up and results, in Table 1 we report the sample preparation procedures, the main laser parameters, and the results for several laser test patterns; values in the table show quite well our system characterization procedure, and clearly show that the optimization of the laser grooving process allowed us to obtain well-fashioned patterns, avoiding, at the same time, any detectable induced damages to the cell.

Table 1. Sample preparation procedure, main process parameters, and results for a set of laser grooved test patterns at 1064 nm.

Chemical treatment	Thermal treatment	Laser power (W)	Translation speed (mm/s)	Electrical width (µm)	Optical width (µm)
HF+RCA	NO	1.25	10	50	38
		1.7	10	60	46
		4.1	10	120	75
		1.7	20	45	35
NaOH 12% 15', 80°C	NO	1.25	10	60	60
		1.7	10	75	75
		4.1	10	165	160
HF+RCA		1.7	20	60	60
NaOH 12% 15', 80°C	YES	1.25	10	65	60
		1.7	10	70	75
		4.1	10	160	160
HF+RCA		1.7	20	60	60

APPLICATIONS.

Our research is devoted to evaluate the feasibility of the laser assisted processes when applied to mono and polycrystalline high efficiency solar cells. In particular, when dealing with polycrystalline silicon, laser applications seem to be a solution to the difficulties connected with this material.

High efficiency devices, texturing, and laser induced doping are the subjects of our studies. The results obtained so far on the use of our system are shown in the next subsections.

High efficiency solar cells. Laser grooved solar cell technology, originally developed elsewhere /3,6/, is one the ways to obtain high efficiency devices (buried contact solar cells). According to this technology, on the surface of a lightly diffused wafer, grooves are opened through a silicon nitride layer by using a laser scriber. After a second heavy diffusion into the grooves, metal contact is formed into the scribes by electroless deposition.

We have used our Nd-YAG laser in the fabrication process of selective emitter, buried contact solar cells on mono and polycrystalline silicon.

After a $POCl_3$ open tube diffusion, we deposited a Si_3N_4 layer by a plasma assisted CVD; then, by using the laser, we scribed grooves through the film, according to the procedure reported above. Subsequently the BSF formation, a Nickel electroless deposition was performed to get the front contact. In conclusion we have shown the feasibility of a silicon solar cell laser based fabrication process, without any detectable performance losses.

Laser texturization. It is well known that, due to the grain disorientation, chemical texturization of polycrystalline material results only in a partial texturing effect: laser texturing of the cell surface is a possible way of overcoming this difficulty. Both a V-grooved or a pyramidal surface structure, in fact, can be obtained simply by closely grooving or by forming a cross-hatched pattern by the laser.

In order to find the best working conditions, we realized several test patterns on polycrystalline substrates, formed by two sets of orthogonal, parallel grooves.

All the adjustable parameters, such as groove pitch (distance between groove axis), lasing power, substrate-to-lens distance and sample translation rate have been varied.

After the laser process, the sample was chemically cleaned to remove melted residues using the following recipe:

NaOH 15% (15°C 30 min) + HCl (5 min)

After the final etch, the height of pyramids was of about 25 µm.

To study the effects of our process, total reflectance measurements have been then performed on the samples using a Perkin Elmer 330 spectrophotometer, the obtained spectrum was then weighted with the solar spectrum to get the effective reflectance of the wafer, according to the formula:

$$Reff = \frac{\int_{\lambda 1}^{\lambda 2} Rmeas(\lambda) N(\lambda) d\lambda}{\int_{\lambda 1}^{\lambda 2} N(\lambda) d\lambda}$$

On top of same sample we deposited also an ARC film, to check the combined effect of such a layer together with the texturing. Typical curves of a good quality laser textured sample with and without an ARC are shown in Fig. 1, the sample being with about 950 Å of SiO on top.

Table 2. Most significant numbers of the laser texturization set up and results with and. without an ARC.

Pattern	Groove Pitch (mm)	R_{eff} %	ARC (Å)	R_{eff} %
V - groove	40	10.0	950, SiO	4.7
	50	13.6	950, SiO	5.8
Pyramid	40	10.5	950, SiO	4.1
	40	10.5	1400, TiO_2	4.3
	40	11.3	800, TiO_2	3.6
	40	11.3	1600, TiO_2	5.2
	50	8.7	950, SiO	3.9
	50	8.7	800, TiO_2	4.4

In Table 2 we report some of the most interesting values obtained, with reflectance spectra reported for samples with a suitable ARC layer deposited on top, as well as some process variables. As it can be seen, laser texturization process lowers the effective reflectance to less than 10%, while the addition of an ARC pushes down this value to about 4%. It is worth noting that TiO_2 layers have been deposited by using a production process facility.

Laser parameters turned out to be slightly different from those reported above. In particular, we varied the slit speed up to 40 mm/s, the repetition rate was 5000 Hz; lens focus was kept at 23 cm and laser power below 2.5 Watts. Values of the pitch, have been continuously varied from 40 to 70 µm.

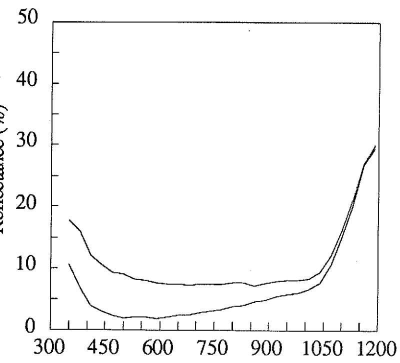

Fig. 1. Reflectance curves for a textured sample with and without (lower curve) an ARC.

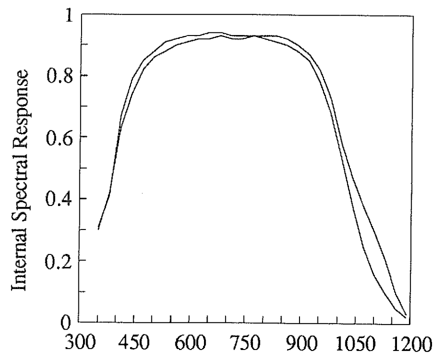

Fig. 2. Internal spectral responses of textured and untextured solar cells.

The use of the 532 nm green light allowed us to get patterns with melted material deposited into the grooves lower than what obtained with the 1064 nm beam; besides, this process gave also smaller pyramids height.

Smaller pyramids made therefore the effective reflectance lowering less efficient; on the other hand, this fact allowed us to test the effectiveness of our process in a screen printed production line, where too high patterns make metal contacts formation impossible.

Still keeping in mind the possible occurrence of laser induced defects, we tested their presence by preparing , on the same wafer, 2x2 sqcm textured and untextured solar cells. On these structures, we then measured the internal spectral response, which is a direct measurements of the changes in the bulk material.

Results are in Fig. 2: there is almost no difference between the two curves, that is, no damage or appreciable change was induced in the material by our laser texturing process.

Laser doping. In an innovative photovoltaic process, doping induced by laser can be applied when needs exist to dope a particular pattern in large area devices.

As an example, no further thermal treatment is necessary in a laser grooved, buried contact, selective emitter cell, as it could be replaced by a localized dopant diffusion induced by the laser. Another example of the applications of laser doping could be the formation of a selective BSF on the rear of the cell.

The basic idea for this process is that, under high fluence pulsed laser irradiation, the surface of the irradiated sample melts, and some material incorporation coming from the surrounding environment takes place /7/.

In our particular experiment, the 532 nm line is used to confine the whole process as close as possible to the surface, so to successfully promote the dissociation of molecules. Moreover, grooving and melting in the same step are achievable. Laser beam contemporary melts the silicon surface and creates dopants by pyrolysis from an adsorbed layer. The incorporation of desired atoms takes place during the melting time, dopants are driven in the liquid phase by fast diffusion. We use PCl_3 as dopant-bearing gas, the wafer is placed into the reaction chamber, and the process starts only after a sufficiently long period of high vacuum cleaning of the environment; the process is performed at a gas pressure of 70 mbar.

Experiments on this subject are still at a preliminary stage, and started from finding a range of laser parameters in such a way to be able to vary from a simply melted line to the usual grooved patterns.

Our goal is to study the properties of the junctions obtained with this method, and to apply it at a high efficiency process.

CONCLUSIONS.

In this paper we have reported the design and the set-up, of a Nd-YAG laser system to be used in solar cells processing. This system has been applied to make buried contacts in high efficiency solar cells, to texture silicon surface, and to obtain laser doped patterns. Results obtained so far are satisfactory, and show the feasibility of this process technique, mainly on polycrystalline silicon.

This work is partially supported by the E.C. in the JOULE II, "Multichess 2" Program.

REFERENCES.

/1/ H. A. Haulich: 10th E. C. Photovoltaic Solar Energy Conference, p. 1124 (Kluwer Academic Publishers, Lisbon 1991)

/2/ L. Quercia, S. Avagliano, A. Parretta, E. Salza and P. Menna: this conference.

/3/ M. A. Green: *High Efficiency Silicon Solar Cells* , p. 169 (Trans Tech Publications, Switzerland 1987).

/4/ D. L. King, B. R. Hansen and W. M. Lehrer: 21st IEEE Photovoltaic Specialists Conference, p. 278 (Orlando 1990).

/5/ A. M. Goodman, J. Appl. Phys. **32**, 2550 (1961).

/6/ M. A. Green: 10th E. C. Photovoltaic Solar Energy Conference, p. 250 (Kluwer Academic Publishers, Lisbon 1991).

/7/ G. G. Bentini, M. Bianconi, L. Correra, R. Nipoti, C. Summonte, C. Cohen and J. Siejka: E-MRS Meeting **15**, 251 (1987).